Journal of Fish Diseases

WILEY

Journal of Fish Diseases

RESEARCH ARTICLE OPEN ACCESS

Metabarcoding Reveals a Potentially Undescribed Columnaris-Causing Bacterium in Peracute Skin Disease of Rainbow Trout (*Oncorhynchus mykiss*, Walbaum)

Samuele Zamparo[1] | Ginevra Brocca[2] | Fabio Marroni[3] | Slobodanka Radovic[4] | Ciro Castellano[1] | Diana Torge[5] | Serena Bianchi[5] | David Groman[2] | Guido Macchiarelli[5] | Luisa Vera Muscatello[6] | Donatella Volpatti[3] | Massimo Orioles[7]

[1]Azienda Agricola Erede Rossi Silvio di Rossi Niccola, Sefro, MC, Italy | [2]Aquatic Diagnostic Services, Atlantic Veterinary College, University of Prince Edward Island, Charlottetown, Prince Edward Island, Canada | [3]Department of Agricultural, Food, Environmental and Animal Sciences, University of Udine, Udine, Italy | [4]IGA Technology Services Srl, Udine, Italy | [5]Department of Life, Health and Environmental Sciences, University of L'Aquila, L'Aquila, Italy | [6]Department of Veterinary Medical Sciences, University of Bologna, Ozzano dell'Emilia, BO, Italy | [7]AULSS 2 Marca Trevigiana, Treviso, Italy

Correspondence: Ginevra Brocca (gbrocca@upei.ca)

Received: 25 March 2025 | **Revised:** 5 June 2025 | **Accepted:** 9 June 2025

Funding: The authors received no specific funding for this work.

Keywords: columnaris-causing bacteria (CCB) | *flavobacterium* | next-generation sequencing (NGS) | rainbow trout | skin disease

ABSTRACT

Columnaris-causing bacteria (CCB) represent a group of four *Flavobacterium* species, previously classified under *Flavobacterium columnaris*, causing a threatening condition in salmonid farming characterised by cutaneous and gill lesions, commonly referred to as 'saddleback disease'. A peracute skin disease outbreak with high mortality in rainbow trout (*Oncorhynchus mykiss*) farms in Northern Italy was investigated. The disease presented with skin discoloration and scale lifting without internal organ abnormalities, leading to a weekly cumulative mortality of up to 80%. The disease was successfully managed with Oxytetracycline treatment, with no relapses observed. Conventional investigation methods produced inconsistent results, prompting additional analyses. Metagenomic sequencing of the 16S rRNA identified *Flavobacterium* species differing from the classical CCB based on the alignment of the V3 and V4 regions, with best matches to *Flavobacterium bernardetii*, *Flavobacterium aquicola*, and *Flavobacterium hiemivividum*. Histopathology and SEM confirmed epidermal necrosis and bacterial infiltration in the dermis, with filamentous bacteria resembling *Flavobacterium* morphology yet differing from classical CCB lesions. These findings point to a previously undescribed *Flavobacterium*-related skin disease with significant economic implications, supporting the value of metagenomic in investigating microbial dynamics in aquaculture diseases, especially in sites exposed to external environments. Further research is required to clarify the pathogenic mechanisms and guide effective management strategies for future outbreaks.

1 | Introduction

Flavobacterium columnare is the causative agent of columnaris disease. This bacterium affects both cultured and wild freshwater fish, including many susceptible commercially important fish genera, such as Salmonids, Cyprinids, Poecilids, Ictalurids, and Cichlids (Decostere et al. 1998; Declercq et al. 2015; Dong et al. 2015; Soto et al. 2008). The disease is mainly characterised by cutaneous and gill lesions ranging from fulminating to chronic progression and causing devastating mortality rates and high economic losses (Declercq et al. 2015; Hadfield 2021).

In recent years, *F. columnare* has undergone reclassification and is now recognised as four distinct species: *F. columnare* (genetic group 1), *Flavobacterium covae* (genetic group 2), *Flavobacterium davisii* (genetic group 3), and *Flavobacterium oreochromis* (genetic group 4); overall, these four species are referred to as Columnaris-causing bacteria (CCB). This reclassification is based on the 16S rRNA and GyrB gene sequences (LaFrentz et al. 2022). Notably, *F. columnare* is highly pathogenic to rainbow trout (*Oncorhynchus mykiss*, Walbaum), while *F. covae* and *F. davisii* exhibit low and moderate pathogenicity to this species, respectively (LaFrentz et al. 2022).

In salmonids, CCB are associated with whitish focal necrotic patches in the gills, fin rot, and skin lesions resembling a saddle starting dorsally and spreading on flanks (Declercq et al. 2015). Systemic disease is common as well (Hadfield 2021; Avendaño-Herrera et al. 2011). The histopathological examination typically reveals epidermal ulceration, necrosis, loss of scales, and deep infiltration of filamentous bacteria, which can result in interstitial inflammation of the hypodermis and myositis (Declercq et al. 2015).

In recent years, the advance of new molecular techniques such as next-generation sequencing (NGS) has improved the investigation of complex events underlying disease outbreaks, finding promising applications in salmonid aquaculture (Birlanga et al. 2022; Zamparo et al. 2024). This method involves sequencing and categorising the genetic material of microorganisms to gain comprehensive qualitative and quantitative insights into the entire sample population. NGS techniques overcome the limitations given by classical diagnostic techniques (such as bacteriology and virology) and provide a much more comprehensive picture of the complicated interaction between organisms, environment, and host (Buermans and den Dunnen 2014). This is particularly true when investigating fish tissue like the skin and gills, which are constantly exposed to the external environment and present a complex and diverse microbiome (Sehnal et al. 2021). Classical bacteriology, which can only isolate microbes that can grow on specific media, can magnify or underrepresent certain bacterial populations based on their ability to grow on a specific medium. Furthermore, a vast majority of bacterial species, known as 'Microbial Dark Matter' (MDM), have not been isolated or described yet (Jiao et al. 2021; Solden et al. 2016; Hutson et al. 2023).

Several limitations of NGS warrant consideration, primarily due to the presence of MDM, which may lead to misinterpretation of results, as well as the need for caution when analysing metagenomic data due to incomplete reference databases and the challenges of identifying species from limited genomic fragments.

This study aimed to characterise high-mortality peracute skin disease outbreaks in rainbow trout farmed in Northern Italy, with clinical features resembling columnaris disease, using an integrated approach based on 16S NGS analysis.

1.1 | General Description of the Case Study

The affected farms are located in three provinces in the Lombardy and Piedmont regions in the North of Italy. They supply water from wells with constant temperatures ranging from 14.5°C to 16°C throughout the year and degas and oxygenate the water before use. All the sites breed fish from eggs to a weight of 10–20 g when they are moved to grow-out facilities.

Starting from summer 2015, these facilities experienced periodical sudden and severe mortality events, with cumulative mortality reaching 30% within the first 3 days and 80% within a week. Affected fish display dorsal areas of skin discoloration and rough texture, resembling columnaris disease, without abnormalities in the internal organs (Figure 1). The disease was successfully managed with oral administration of Oxytetracycline at a daily dose of 120 mg/kg for 10 days. The antibiotic dose and administration regimen were selected and monitored by the responsible veterinarian, taking into account the outbreak severity, the failure of lower doses of the drug to resolve the event, recent studies showing the safety of this drug at the given dose (Leal et al. 2019), and the optimal administration regimen in fish to maximise the drug's efficacy (Rigos et al. 2021). The treatment in all cases resolved the mortality without further relapses in the same batch.

Fish affected by the disease were repeatedly submitted to bacteriological analyses performed on Columbia Blood Agar and Anaker Ordal Agar (Buller 2014) and identified as described in Zamparo et al. 2024. The bacterial isolation results were variable from time to time, and there were no constant isolates among different outbreaks. The isolated bacteria were *Pseudomonas* spp., *Aeromonas sobria*, *Aeromonas veronii*, *Acinetobacter* spp., *Cryseobacterium* spp., *Carnobacterium maltaromaticum*, *Citrobacter* spp., *Flavobacterium psychrophilum*, *F. columnare*, and other *Flavobacterium* spp. Histological analyses were able to describe the pathological change affecting the fish, but could only identify a mixed bacterial population, including filamentous bacteria, affecting the epidermis.

Overall, these findings suggested a bacterial skin infection of undefined aetiology. Further investigations were conducted to clarify the origin of these mortality outbreaks, including a 16S NGS analysis, virological, scanning electron microscopy, and histological examinations. The present manuscript refers to an outbreak that happened in one of the facilities in November 2022.

2 | Material and Methods

2.1 | Water Quality and Environmental Parameters

A static monitoring implant continuously monitored oxygen and temperature at the investigated site. Total Gas Pressure (OxyGuard International A/S; Farum, Denmark; https://www.oxyguard.dk/en/product-overview-probes/tgp-probe/) and CO_2 (OxyGuard International A/S; Farum, Denmark; https://www.oxyguard.dk/en/product-overview-hand-held-portable/co2-analyzer/) were measured every other week.

2.2 | Fish Sampling

Fish samples were taken before (named 'T0' sampling time point) and after (named 'T1' sampling time point) the Oxytetracycline treatment (Figure 2). All fish were humanely

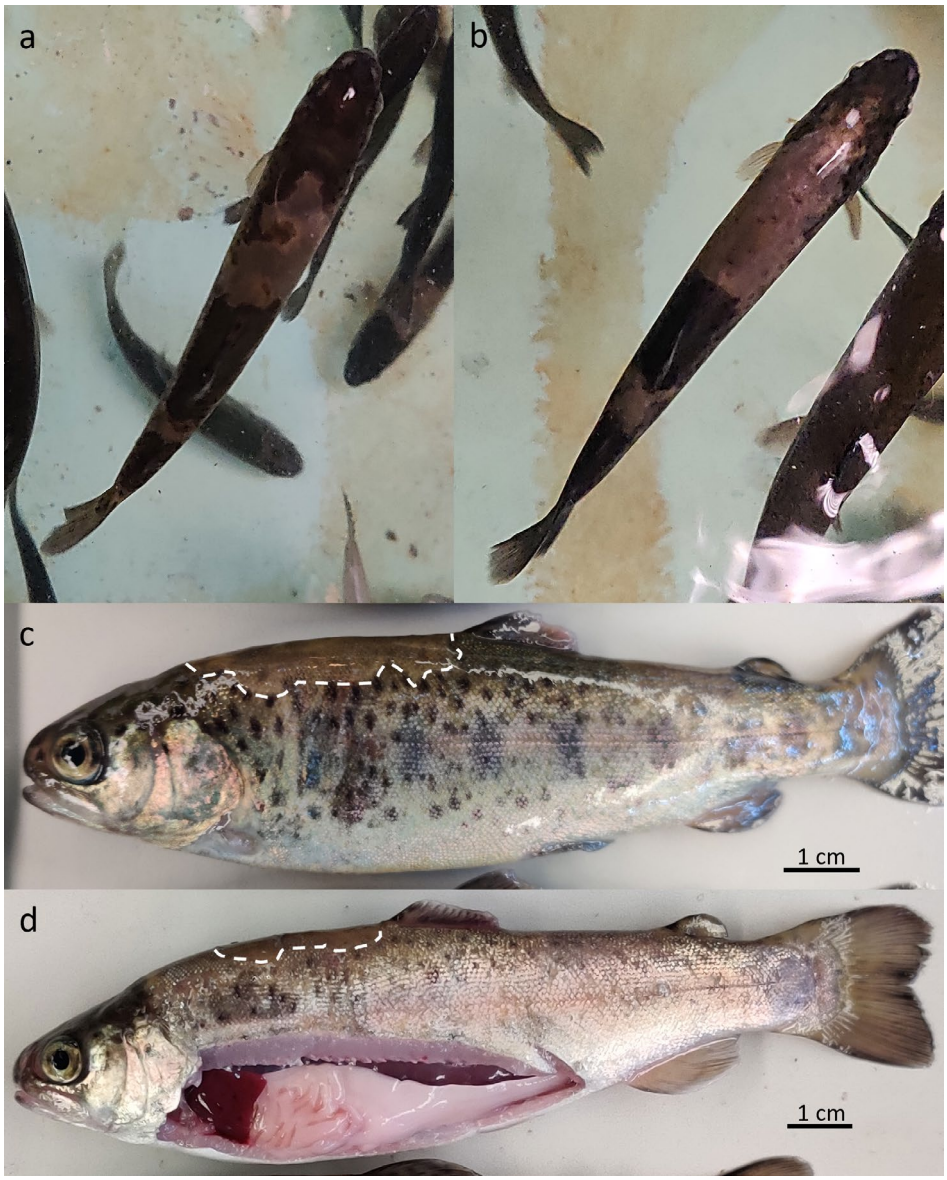

FIGURE 1 | Affected fish from the 'Moribund T0' group. (a, b) Dorsal view of affected rainbow trout (*Oncorhynchus mykiss*) in the tanks, showing locally extensive and well-defined areas of skin discoloration on the back. (c, d) Necropsy exam. (c) External appearance of affected fish after removal from the tanks. (d) Opening of the coelomic cavity reveals no significant macroscopic alterations. In both c and d, the dashed line outlines the affected areas.

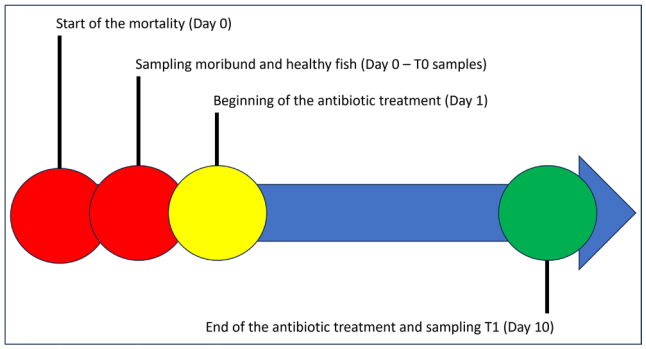

FIGURE 2 | Timeline of the samplings and antibiotic treatment.

euthanised with tricaine methanesulfonate (Tricaine, Pharmaq) at a concentration of 0.6 g/L until the complete absence of opercular movement.

2.3 | Necropsy, Wet Mounts, and Histology

Routine wet mounts and necropsies were performed in the field on the moribund fish at T0. Wet mounts were prepared by scraping the skin with the glass coverslips and pressing the coverslip onto the histological slide using a drop of physiological solution. The gills were analysed by cutting the filaments at the base, placing them on a histological slide with a drop of physiological solution, and pressing them with a coverslip. For all samples taken, necropsies were performed in two steps: macroscopic evaluation of the gills and the integument, and after opening of the coelomic cavity, macroscopic observation of the internal organs (Noga 2010). Four moribund fish were sampled at T0 and fixed as a whole in 10% neutral buffered formalin (NBF) for at least 48 h for histological analysis. Transverse and sagittal sections of the fish, including the affected body walls and main organs, were then trimmed in biocassettes, dehydrated in ethanol series, and embedded in paraffin.

Tissue sections were cut at 4 μm with a microtome and stained with haematoxylin and eosin (H&E) and Methylene Blue staining.

2.4 | Virology

A pool of moribund fish was taken for virological analyses at the T0 sampling time point. Portions of the head kidney, spleen, heart, and brain were collected from fish before the treatment and pooled for biomolecular analysis targeting Infectious Haematopoietic Necrosis virus (IHNv), Viral Haemorrhagic Septicemia virus (VHSv), and Salmonid Alphavirus (SAV). The samples were manually ground with sterile quartz sand. Minimum Essential Medium (MEM) was added to obtain a 1:3 w/v dilution. The homogenised sample was centrifuged at 8000 g for 2 min, and the supernatant was collected. Total nucleic acids were extracted from 250 μL of supernatant using QIAsymphony DSP Virus/Pathogen Midi Kit (Qiagen) and the automated QIAsymphony SP (Qiagen) system. Isolation of the nucleic acids was performed following the manufacturer's recommendations. Real-time RT-PCR was employed to detect IHNv, VHSv, and SAV (Overturf et al. 2001; Jonstrup et al. 2013; Hodneland and Endresen 2006).

2.5 | Scanning Electron Microscopy

Skin samples for scanning electron microscopy were taken from the Moribund T0 fish group. Skin samples were preserved in 2.5% Glutaraldehyde (Agar Scientific, Cambridge Road Stansted Essex, UK) in PBS (primary fixation) and stored at 4°C (Orioles et al. 2022). After the lab received them, the samples were washed in PBS (0.1 M, pH 7.2) three times, for 30 min each time (renovating the PBS each time) and post-fixed with 1% Osmium tetroxide (OsO_4) (Agar Scientific, Stansted, UK) in distilled water for 2 h (Torge et al. 2024). Samples were then rewashed in PBS three times for 10 min each time (renovating the PBS each time) and dehydrated in an ascending series of ethanol solutions: 30% (10 min), ethanol 50% (10 min), ethanol 70% (10 min), ethanol 80% (10 min), 90% (10 min), ethanol 95% (10 min, twice) and ethanol 100% (15 min, four times). The samples were then immersed in 100% hexamethyl-disilane (HDMS, Sigma-Aldrich S.r.l., Milan, Italy) for 3 min and air-dried. After transferring the samples into a desiccator to prevent water contamination, the covered glasses were mounted on metal stubs, gold stained, and then observed using SEM (GEMINI_SEM, ZeisFInals, Germany) at different magnifications, using secondary electron probes.

2.6 | 16S rRNA NGS Sampling and Analysis

For NGS analysis, sampled fish were frozen at −20°C as a whole. The sample included four moribund fish with evident focal discoloration of the back (named 'Moribund T0') and four apparently healthy fish from the same tank without any evident lesion (named 'Healthy T0'). After 10 days of treatment with oxytetracycline, when the mortality resolved, four fish were sampled at T1 (Figure 2).

All samples (12 specimens in total) were transported in dry ice to the IGAtech lab (Udine, Italy), where metagenomic analyses were performed. Samples were thawed, and a very thin slice of skin from the affected area (or from the dorsal part of the fish, anterior to the dorsal fin in healthy specimens) was collected using a disposable scalpel blade.

Serum and stool protocol of Mag-BindUniversal Pathogen 96 Kit (Omega Bio-tek, Norcross, GA) for tissue samples was used for DNA extraction with minor modification of the initial step: for each sample, 100 mg of skin was resuspended in 500 μL SLX-Mlus buffer and homogenised with an iron bead (Qiagen, Hilden, Germany) by vortexing at max speed for 2 min on a Tissuelyser (Qiagen, Hilden, Germany). Subsequently, 300 μL of lysate was collected and vortexed at maximum speed for 5 min to lyse the samples with lysis buffer and Proteinase K. The final elution was done with 50 μL of 10 mM Tris–HCl.

Libraries were prepared by following the Illumina 16S Metagenomic Sequencing Library Preparation protocol in two amplification steps: an initial PCR amplification using locus-specific PCR primers with overhangs 16S-341F 5′-TCGTCGGCAGCGTCAGATGTGTATAAGAGACAGCCTACGGGNGGCWGCAG-3′ and 16S-805R 5′-GTCTCGTGGGCTCGGAGATGTGTATAAGAGACAGGACTACNVGGGTATCTAATCC-3′, and a subsequent amplification that integrates relevant flow-cell binding domains and unique indices (NexteraXT Index Kit, FC-131-1001/FC-131-1002). PNA clamping was applied during the first amplification step to block host mitochondrial 16S sequence amplification following the manufacturer's protocol (PNA Bio Inc., Newbury Park, CA). Libraries were sequenced on a NovaSeq 6000 instrument (Illumina, San Diego, CA) in paired-end 250-bp mode.

2.7 | Bioinformatics Analysis

Masking of sequencing adapters was performed by the sequencing service provider. To remove host mitochondrial 16S sequences, reads were filtered using bbduk (https://sourceforge.net/projects/bbmap/) using *O. mykiss* reference assembly (https://www.ncbi.nlm.nih.gov/datasets/genome/GCF_013265735.2/). Filtered reads were classified using Kraken2 with default parameters (Wood et al. 2019) on the 16S curated RefSeq database (https://www.ncbi.nlm.nih.gov/refseq/targetedloci/16S_process/) at the species and genus level. All subsequent analyses were performed at the taxonomic level of species and genus.

Abundance estimation was refined using bracken (Lu et al. 2017) with the following parameters:

1. The threshold was set to 10 reads. The threshold is the minimum number of reads attributed by kraken2 to taxa to perform taxa abundance estimation with bracken2. This step was used to remove extremely rare taxa from the analysis.
2. The read length was set to 250. This corresponds to the length of the reads after the sequencing facility removed adapters.

Species relative abundance is reported as percent of sequenced reads belonging to the species (Cattonaro et al. 2018); in addition, species relative abundance is also reported as number of reads belonging to each species, normalised using the varianceStabilizingTransformation function implemented in DESeq2 (Love et al. 2014).

Alpha diversity was assessed using the R package vegan (https://CRAN.R-project.org/package=vegan); beta diversity was assessed using PERMANOVA implemented in the adonis2 function of the vegan package. Differential abundances were assessed using DESeq2 (Love et al. 2014).

Differential abundance results for the 'Moribund T0' VS 'Healthy T0' and 'T1' comparisons were filtered to remove false positives due to rare taxa. Results were considered only for species satisfying the following criteria:

1. The number of reads assigned to a taxon in the two groups must be at least 300.
2. At least one read must be assigned to the taxon in at least three samples (representing the 50% + 1 of a single group).

Results of the differential abundance were sorted by false discovery rate (FDR). Taxa with FDR $< 10^{-3}$ were prioritised in the presentation and discussion of the results.

An independent analysis using fastANCOM (Zhou et al. 2022) was also performed to validate the differential abundance results obtained with DESeq2. Both methods identified similar major taxa as differentially abundant, with some variations in taxa with lower representation, but the results overlapped. Since DESeq2 is widely used for metagenomic differential abundance analysis and ensures high sensitivity, we present our main findings based on this approach.

To exclude potential misassignments based on the best match criterion, specific *Flavobacterium* species reference sequences from the RefSeq database were aligned to minimise the likelihood that the *Flavobacterium* species detected in our study were mistakenly identified as *F. columnare*, *F. covae*, *F. davisii*, or *F. oreochromis*, which are known as the CCB. To do so, RefSeq database sequences were extracted and compared using Clustalw (https://www.genome.jp/tools-bin/clustalw).

2.8 | Ethics Statement

This study monitored a natural infection and subsequent antibiotic treatment as part of routine diagnostic procedures in a commercial fish farm. As per Directive 2010/63/EU of the European Parliament and of the Council of 22 September 2010, regarding the protection of animals used for scientific purposes, the Italian legislation (D. Lgs. n. 26/2014) does not require approval from ethics committees for the use of samples submitted or taken for diagnostic purposes.

3 | Results

3.1 | Water Quality and Environmental Parameters

During the study, the dissolved gases were within optimal ranges for trout farming (oxygen sat > 80%; residual gases < 104%; CO_2 < 10 ppm), the temperature ranged from 14.5°C to 15°C, and the pH was stable at 7.6.

3.2 | Necropsy, Wet Mounts, and Histopathology Findings

At T0, observations of the gills and wet skin mounts showed no pathological alterations or presence of parasites.

Macroscopic findings in the 'Moribund T0' fish included the sole presence of locally extensive areas of discoloration on the fish's back, which exhibited a rough texture to the touch. The lesions were clearly visible when observing live fish in the rearing tanks (Figure 1a,b), while lesions were more difficult to appreciate in dead animals examined out of water (Figure 1c,d). At the opening of the coelomic cavity, no alterations of the internal organs were visible (Figure 1d).

Microscopically, subgross magnification of the specimens from the 'Moribund T0' group revealed multifocal extensive areas of the dorsal skin showing prominent ectasia of the scale pockets and eversion or loss of the scales (lepidorthosis) (Figure 3a,b). High magnification of affected areas showed sloughing and necrosis of the epidermal layer in the affected areas, exposure of the superficial dermis, loss of scales, and ectasia of the scale pockets. The lesions were characterised by sharp margins, reflecting the well-defined borders detected macroscopically (Figure 4a). The denuded superficial dermis showed moderate edema and was multifocally infiltrated by clusters of mixed bacteria, most of which had filamentous morphology (Figure 4b,c). The adjacent skin presented a generalised thinning of the epidermis, with reduced goblet cells and elongation of the superficial epithelial cells. No significant morphological alterations were observed in the other organs. Many filamentous bacteria were visible within the affected superficial dermis and scale pockets using the methylene blue stain, associated with fewer plump rod-shaped bacteria (Figure 4d,e). No evidence of inflammatory infiltration was detected, and the final diagnosis was of peracute, locally extensive, severe epidermal necrosis with intralesional bacteria.

3.3 | Virology

The virological analysis yielded negative results for VHSv, IHNv, and SAV.

3.4 | SEM

SEM analysis revealed numerous colonies of microorganisms in the scale pockets (Figure 5). These microorganisms were long, slender, and rod-shaped, approximately 0.3–0.5 μm wide and 3–8 μm long (Figure 5).

3.5 | NGS and Bioinformatic Analysis

Samples were clustered using principal component analysis (PCA, Figure 6). One sample from the T1 group exhibited a distinct clustering pattern, suggesting a deviation from the rest of the group. A Bray-Curtis distance analysis was performed using SciPy (version 1.9.3) in Python to validate this further. This sample had a mean Bray-Curtis dissimilarity of 0.46 compared to the other T1 samples. This deviation indicates a distinct microbial composition that

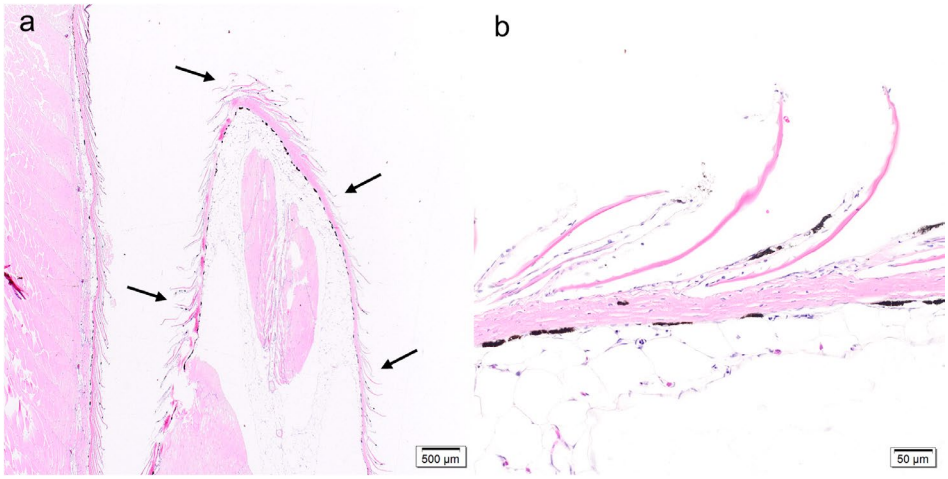

FIGURE 3 | Subgross appearance of the affected areas. (a, b) Diffuse loss of the epidermis and eversion of the scales (arrows). (b) Higher magnification of (a).

could introduce bias in downstream analyses. Consequently, the sample was excluded from subsequent analyses to ensure group coherence and statistical reliability. Nonetheless, its removal did not substantially impact the overall results.

The total number of reads obtained from the samples averaged 1,632,244 reads per sample (min: 988,106; max: 2,325,650). After filtering host-derived sequences, we retained 152,206 reads from the 'Healthy T0' group, 432,147 from the 'Moribund T0' group, and 349,766 from the 'T1' group, with a mean of 84,919 reads per sample.

PCA revealed a clear separation among the three groups, with the first principal component explaining 28% of the total variance and the second principal component accounting for 15%. Moribund T0 samples were distinct from both Healthy T0 and T1 along the first component, whereas Healthy T0 and T1 were primarily separated along the second component, suggesting lower diversity within these groups compared to Moribund T0.

PERMANOVA confirmed significant differences in microbial composition across groups ($p = 0.0005$), with group identity accounting for 54.07% of the variance in the distance matrix. A major shift in microbial composition was observed between Moribund T0 and T1 (47.4% variance explained, $p = 0.0286$), suggesting treatment-induced changes. Significant differences were also detected between Healthy T0 and Moribund T0 (36.2% variance explained, $p = 0.0307$), as well as between Healthy T0 and T1 (32.7% variance explained, $p = 0.0286$).

Alpha diversity analysis revealed significant differences between groups in both diversity and species richness (Figure 7). The Simpson's and Shannon's indices were lower in the Moribund T0 group compared to Healthy T0 and T1, indicating reduced microbial diversity during disease. In contrast, species richness and Chao1 index did not show significant differences between Healthy T0 and Moribund T0, suggesting that the disease did not drastically reduce the total number of taxa but rather altered their relative abundances.

After treatment (T1), species richness and Chao1 index increased compared to both Healthy T0 and Moribund T0, suggesting the emergence of new taxa. On the other hand, Simpson's and Shannon's indices in T1 remained similar to Healthy T0, suggesting that while new taxa appeared, their low abundance did not significantly alter the overall microbial diversity. These results suggest that while the treatment promotes colonisation by new taxa, the community structure remains comparable to the pre-disease state in terms of diversity.

The comparison of the various groups' NGS results on the genus level (Figure 8) showed that the only statistically significant varying genus between the 'Healthy T0' and 'T1' groups was *Acetobacter* with a FDR of 7.99×10^{-19}. This genus was present only in the post-treatment group and represented only 1.17% of the reads.

In the comparison between the 'Healthy T0' and the 'Moribund T0' groups, the only two genera with a statistically significant variation were *Flavobacterium* with a FDR of 1.06×10^{-9}, representing 0.43% of the reads in 'Healthy T0' and 68.75% in the 'Moribund T0' groups, and *Polaribacter* with a FDR of 7.68×10^{-8}, not present in 'Healthy T0' group and representing 1.22% of the reads in the 'Moribund T0' group.

The comparison between the 'Moribund T0' and 'T1' groups highlighted statistically significant variation only for the *Flavobacterium* genus, with a FDR of 1.75×10^{-6}, representing 0.47% of the reads in the 'T1' group.

Before the treatment, the most represented bacterial genera in the 'Healthy T0' group were *Burkholderia*, *Succinovibrio*, and *Prevotella*, respectively, 33.6%, 9.7, and 5.9% of total reads (S.T1, Data S1). A very similar scenario was found in the 'T1' group (S.T2, Data S1). *Burkholderia* represented 40.13% of the total reads, while *Succinovibrio* and *Prevotella* were 8.9% and 3.1%, respectively. In the 'T1' group, the genus *Sphingomonas* also had more than 5% reads. A very different scenario characterised the 'Moribund T0' fish (S.T3, Data S1). The most prevalent bacteria of the 'Healthy T0' and 'T1' groups appeared to be poorly represented in the 'Moribund T0' fish, except the *Burkholderia* genus, representing 11.35% of the total reads, and the vast majority of reads were represented by the *Flavobacterium* genus, representing 68.75% of total reads. Most of these flavobacteria reads were aligned in our analysis at the species level with *F.*

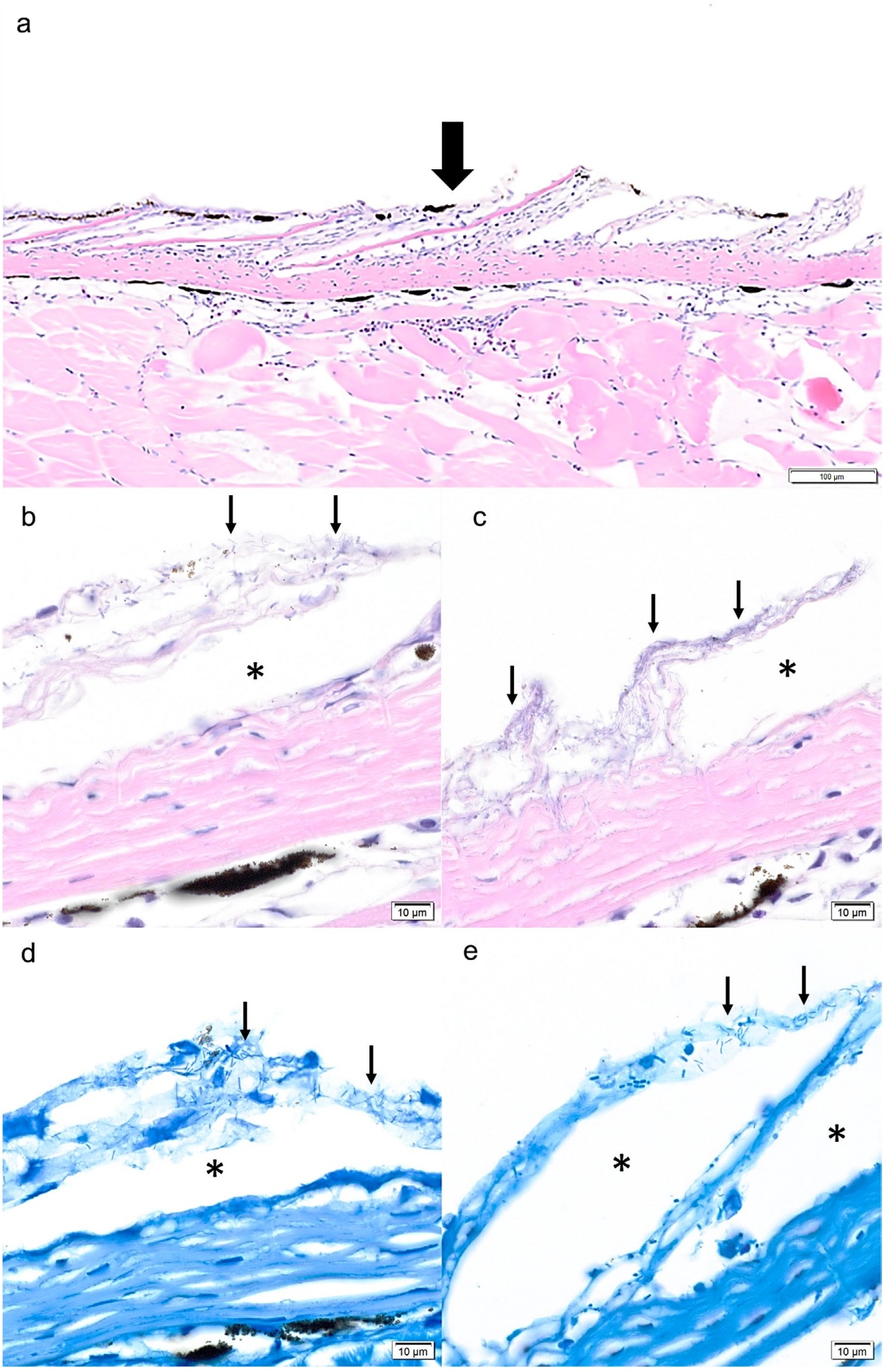

FIGURE 4 | Legend on next page.

FIGURE 4 | Microscopic appearance of the affected skin. (a) High-power view showing a sharp transition (thick arrow) between the affected areas (right), characterised by epidermal loss and scale pockets ectasia (*), and the adjacent skin (left), which appears thinned but otherwise unaffected. Haematoxylin–Eosin (HE). (b, c) Numerous filamentous bacteria (thin arrows) infiltrating the superficial dermis forming the scale pockets (*). Scattered, plump, rod-shaped bacteria are also visible. HE. (d, e) Filamentous bacteria (thin arrows) are highlighted by the special stain (* indicates scale pockets). Methylene Blue.

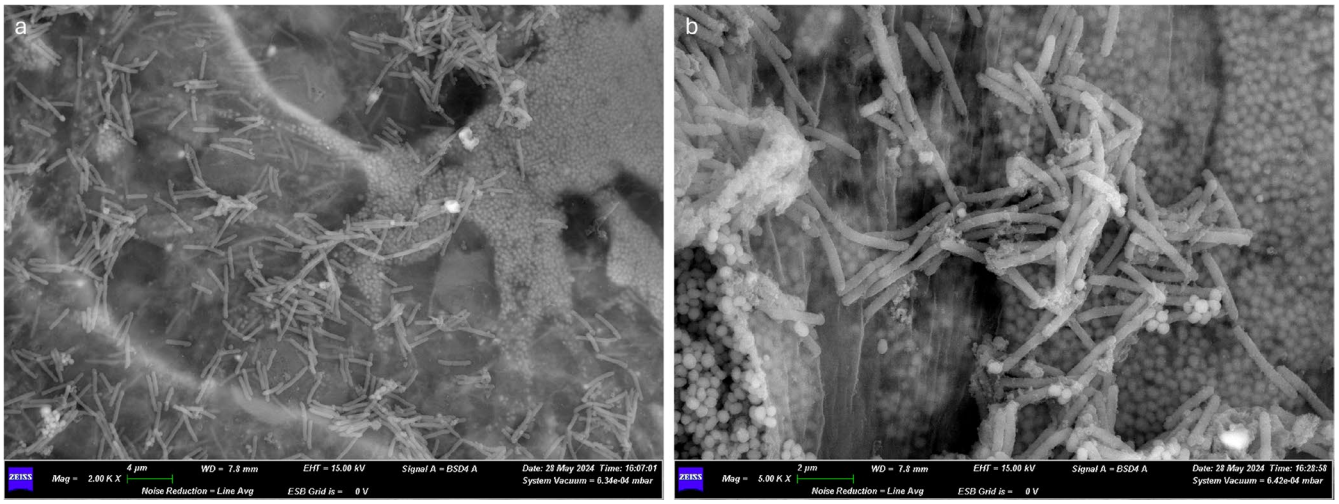

FIGURE 5 | Scanning Electron Microscopy (SEM) micrographs of skin samples. (a) The presence of long, slender, rod-shaped bacteria forming aggregates within the scale pocket was detected through SEM (Magnification: 2.00 K X; Scale bar 4 μm). (b) Higher magnification—the bacteria were approximately 0.3–0.5 μm wide and 3–8 μm long (Magnification: 5.00 K X; Scale bar: 2 μm).

bernardetii (38.1% of the reads), *F. aquicola* (15.7% of the reads), and *F. hiemivividum* (11.7% of the reads).

At the species level, in the comparison between the 'Healthy T0' and 'T1' groups, only three bacterial species showed significant variation. These were aligned through the best match with *Burkholderia vietnamiensis*, *Sphingomonas panni*, and *Bradyrhizobium ferriligni* with a FDR of 1.09×10^{-5}, 1×10^{-3}, and 1.8×10^{-3}. None of these species were found in the 'Healthy T0' group, and they were minimally represented at 'T1' with 4.5%, 1.1%, and 0.7% of the total reads, respectively.

In the comparison between 'Healthy T0' and 'Moribund T0', 12 bacterial species varied with FDR $<10^{-3}$ and these were *F. bernardetii* (FDR 6.4×10^{-9}), *F. psychrophilum* (FDR 3.7×10^{-6}), *Polaribacter gangjinensis* (FDR 8.8×10^{-6}), *F. swingsii* (FDR 1.2×10^{-5}), *F. tegetincola* (FDR 1.4×10^{-5}), *F. sangjuense* (FDR 1.5×10^{-5}), *F. hercynium* (FDR 2.8×10^{-5}), *F. aquicola* (FDR 1.9×10^{-4}), *F. panaciterrae* (FDR 7.6×10^{-4}), *F. hauense* (FDR 5×10^{-3}), *F. sasangense* (FDR 5.7×10^{-3}), and *F. hiemivividum* (FDR 6×10^{-3}).

Most of these species were found only in the 'Moribund T0' group, while no reads were detected in the 'Healthy T0', except for *F. bernardetii*, *F. aquicola*, and *F. hiemivividum* for which a single sample in the 'Healthy T0' group showed few reads. Aside from *F. bernardetii*, *F. aquicola*, and *F. hiemivividum*, all others were poorly represented (max 1.2% of total reads in the moribund group).

In the comparison between 'Moribunds T0' and 'T1' 13 species showed variation with FDR $>10^{-3}$, and these were *F. aquicola* (FDR 1.1×10^{-25}) *Sphingomonas yantingensis* (FDR 2.4×10^{-13}), *Sphingomonas echinoides* (FDR 8.1×10^{-13}), *F. psychrophilum* (FDR 7×10^{-6}), *B. vietnamiensis* (FDR 9.5×10^{-6}), *F. swingsii* (FDR 2×10^{-5}), *F. hercynium* (FDR 4.9×10^{-5}), *S. panni* (FDR 7.3×10^{-4}), *F. panaciterrae* (FDR 9.8×10^{-4}), *B. ferriligni* (FDR 1.3×10^{-3}), *F. bernardetii* (FDR 2.2×10^{-3}), *F. hauense* (FDR 5×10^{-3}), *F. sasangense* (FDR 5.2×10^{-3}), and *F. sangjuense* (FDR 8.3×10^{-3}). Among these species, all the *Flavobacterium* were more prevalent in the 'Moribund T0'; in contrast, the other bacterial species were more concentrated in 'T1' specimens.

F. hiemivividum, besides being well represented in the moribund group, did not show such significant variation (FDR 2.9×10^{-2}).

The results of sequence comparisons through ClustalW are shown in Table 1. This comparison aimed to understand the likelihood of misidentification in our analysis of the most prevalent and statistically significant species with the CCB (*F. columnaris*, *F. covae*, *F. davisii*, and *F. oreochromis*). To do so, all *Flavobacterium* V3-V4 sequences of 16S rRNA were extracted from the database and aligned to understand the similarity among these and the number of intermediate sequences with more likeness of alignment with the best match criterion. The sequence similarity among these most significant species in our analysis has also been investigated, and the results show that *F. bernardetii* and *F. aquicola* share 93% sequence similarity, *F. bernardetii* and *F. hiemivividum* share 94% of sequence similarity, while *F. hiemivividum* and *F. aquicola* share 96% of sequence similarity.

4 | Discussion and Conclusions

This study reports a recurring, highly fatal peracute skin disease affecting rainbow trout, with clinical features resembling

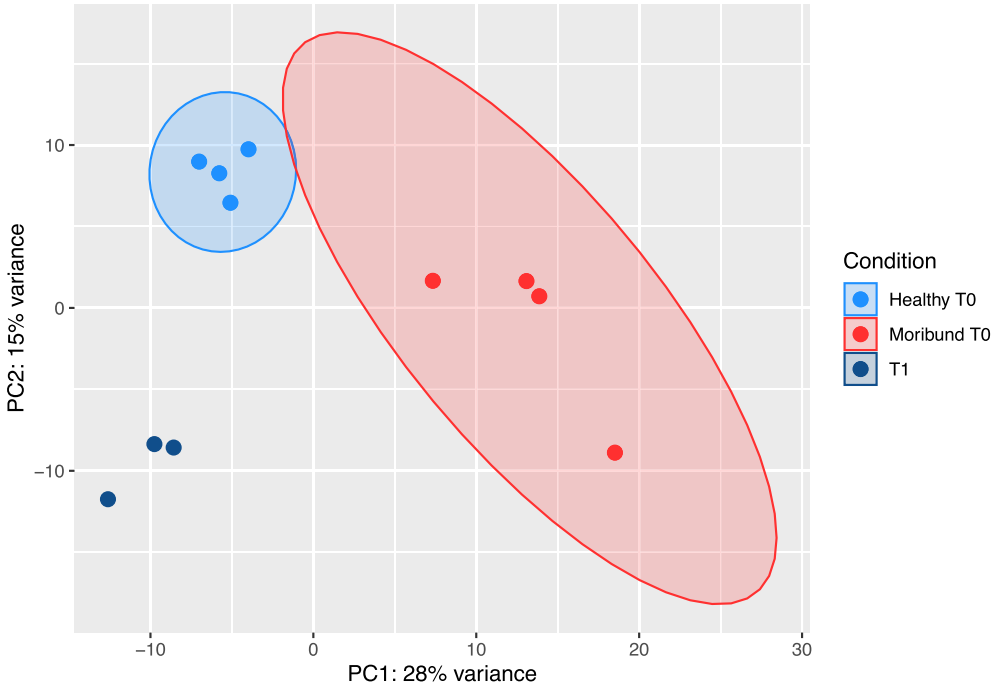

FIGURE 6 | Principal component analysis (PCA) based on skin microbiome composition.

columnaris disease and leading to substantial economic losses. It provides a comprehensive characterisation of the disease, including macroscopic, microscopic, and ultrastructural aspects, and integrates NGS data for further insights.

Similar cases have likely been reported in the past but were not investigated with the same level of detail and characterisation. For example, 'no-mucus skin disease' (Ferguson et al. 1995) closely resembles our case, particularly in its histological presentation. Such previous studies focused on histology, electron microscopy, and bacteriology, and while they lacked a definitive diagnosis, their conclusions aligned with ours, suggesting a bacterial aetiology. However, due to methodological limitations, they were unable to precisely identify the causative agent.

The most distinctive feature of the outbreak described in the present study, which enabled rapid identification by farmers and veterinarians, was the presence of discoloured skin spots with a rough texture.

Histological analyses allowed the identification of the main skin lesions, with sloughing of the epidermal layer and colonisation of the superficial dermis by filamentous bacterial clusters. This was associated with lepidorthosis, characterised histologically by scale lifting, which exposed the underlying dermis. The intralesional filamentous bacteria were more visible and recognisable with Methylene Blue staining rather than HE, and its use is recommended in cases where these agents are suspected. No signs of inflammation were noted, and the findings were consistent with a peracute pathology that likely impacted the health of the fish by altering their osmoregulatory balance through the affected skin. No significant histological changes were detected in any of the internal organs, leaning towards this interpretation.

SEM observations confirmed the presence of mainly long, slender, and rod-shaped microorganisms, which formed aggregates in the scale pockets (Figure 5). This ultrastructural evidence is aligned with histological findings and previous studies, reporting the tendency to aggregation by CCB rather than distributing evenly across the epithelium (Declercq et al. 2013). SEM evidence presented here revealed that these microorganisms were approximately 0.3–0.5 μm wide and 3–8 μm long (Figure 5). These ultrastructural details align with previous ones detecting the presence of bacterial cells 0.3–0.5 μm wide and 3–10 μm long in the gill arch of rainbow trout affected by CCB (Bullard et al. 2011).

The overall comparisons between 'Moribund T0' and the other groups highlighted the presence of the genus *Flavobacterium* as the most important entity in describing the variation between groups, representing more than 68% of the bacterial populations in the 'Moribund T0' group and less than 0.5% in the others.

Three different *Flavobacterium* species are of particular interest based on their relative presence in the sick group and the FDR of the variation of these populations between 'Healthy T0' and 'Moribund T0', and 'Moribund T0' and 'T1' groups. These three species are *F. bernardetii*, *F. aquicola*, and *F. hiemivividum*.

The relative abundance of each taxon, as estimated by the percentage of reads, does not necessarily reflect the true number of bacterial cells due to biases introduced during DNA extraction, PCR amplification, and sequencing. However, previous benchmarking studies using mock communities have shown that, especially for highly abundant taxa, read proportions can serve as an acceptable proxy for biological abundance (Cattonaro et al. 2018).

All other *Flavobacteria* found in this study were considered less important due to their very poor representation compared to these three species.

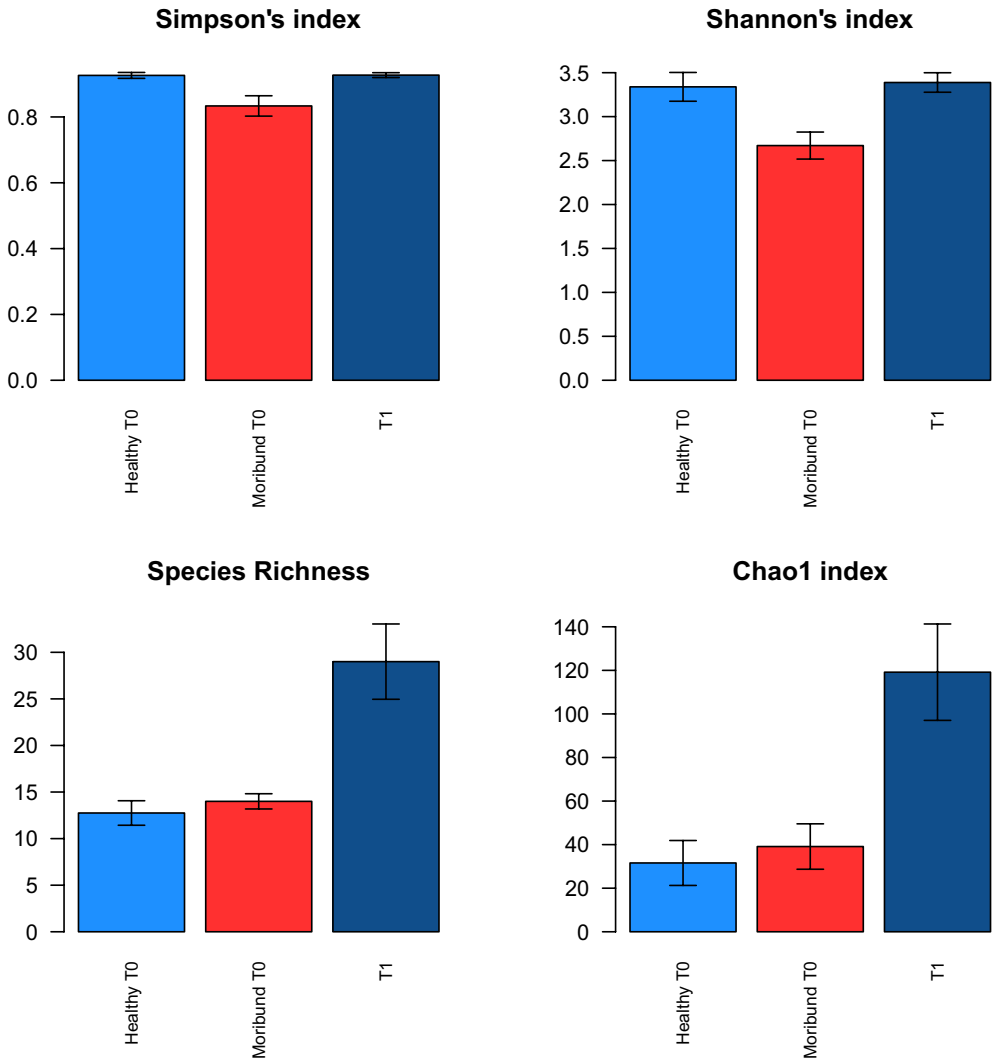

FIGURE 7 | Alpha diversity values in healthy and moribund fish at T0, and in fish at T1. Bar heights represent average values, and whiskers represent standard errors.

To characterise the bacterial community, we employed 16S rRNA V3–V4 fragment sequencing using NGS. Taxonomic assignments were performed through a best-match approach, aligning NGS-derived reads to the RefSeq database. This method relies on sequence similarity and does not provide definitive species-level identification, as closely related species may share highly similar 16S sequences.

To address this limitation, we evaluated the potential misclassification of known CCB, including *F. columnare*, *F. covae*, *F. davisii*, and *F. oreochromis*. Specifically, we extracted all available *Flavobacterium* V3–V4 sequences from RefSeq and compared them across the database. Our analysis revealed that *F. bernardetii* shares higher sequence similarity with 58 other species than with the CCB. Similarly, over 100 species were found to be more closely related to *F. aquicola* and *F. hiemivividum* than to the CCB. These findings allow us to reasonably rule out the direct involvement of known CCB in this outbreak. However, we acknowledge the inherent limitations of 16S-based species identification, which prevent us from excluding the potential role of other, closely related *Flavobacterium* species.

An intriguing collateral finding in this study concerned the sampling methodology for NGS. Although the analysis specifically targets bacterial 16S rRNA, a significant portion of the reads obtained were host reads, which had to be removed before conducting the statistical analysis. In this study, a very thin slice of skin from the lesion area was sampled, yet this approach led to a substantial number of rainbow trout reads, complicating the analysis.

For future NGS analyses of fish skin microbiomes, especially in cases involving superficial lesions like those in this study, swabbing or scraping as sampling methods should be considered to minimise this issue (Clinton et al. 2021).

An additional observation from this study was the almost complete absence of the *Flavobacterium* genus in healthy fish populations ('Healthy T0' and 'T1').

In a previous study by the same authors (Zamparo et al. 2024), treatment with oxytetracycline, administered at the same dosage as in the present report, did not result in a significant

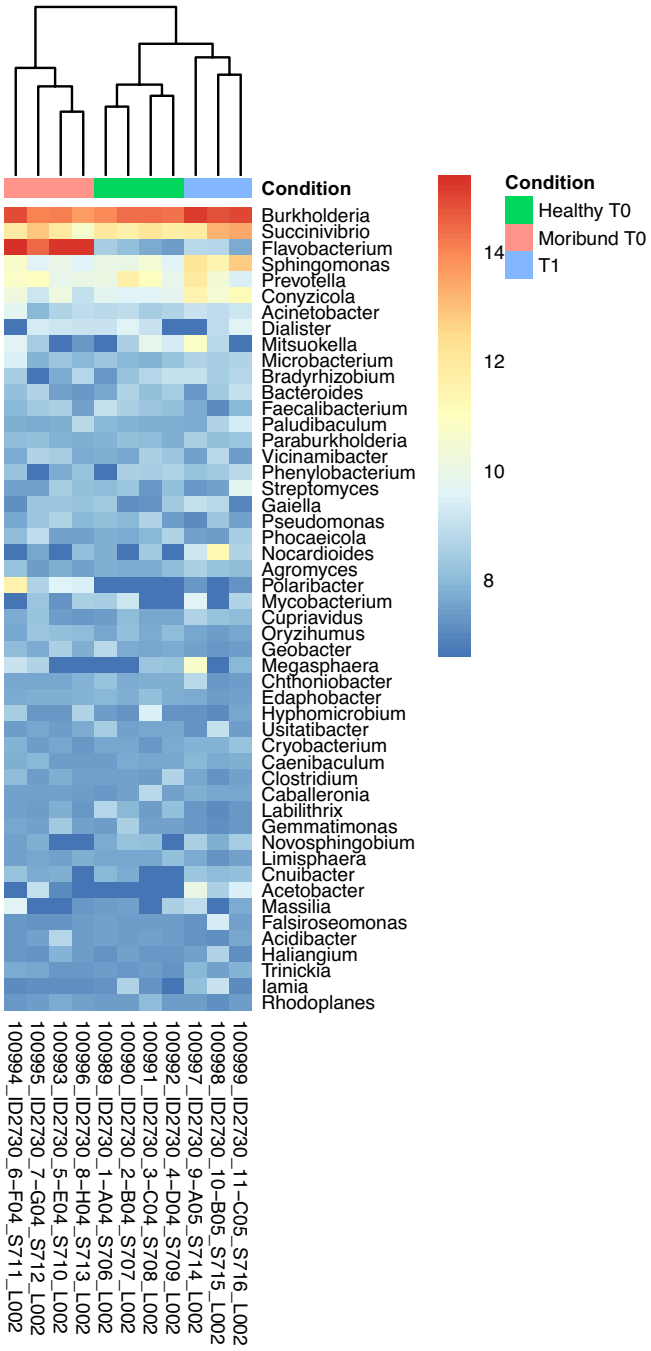

FIGURE 8 | Heatmap and hierarchical clustering based on the 50 most abundant genera ordered by their total abundance from highest (top) to lowest (bottom). The colours of the cells indicate the relative number of reads assigned to a species in every sample (normalised abundance, blue = low abundance, red = high abundance).

reduction of *Flavobacterium* abundance during a gill disease outbreak likely related to environmental factors. Consequently, the effectiveness of the treatment could not be associated with a decrease in the prevalence of this genus. The authors wonder whether the *Flavobacterium* genus, aside from known pathogenic species, exhibits strictly opportunistic behaviour in trout farming and speculate that their presence might serve as an indicator of fish health and welfare, as it appears to be virtually absent in healthy specimens.

To further explore this hypothesis, it would be necessary to conduct the same NGS analysis on fish batches entirely free of mortality and clinical signs of disease, to evaluate the overall prevalence of the *Flavobacterium* genus in healthy populations.

Our results suggest that this outbreak represents a high-mortality condition with clinical and pathological features resembling Columnaris disease in rainbow trout yet involving a different bacterial species.

Several key differences set this outbreak apart from classical Columnaris disease. These include subtle variations in histological presentation, as the skin has never been found ulcerated or haemorrhagic (Declercq et al. 2015), the absence of systemic involvement (Hadfield 2021), the absence of gill-associated clinical signs or fin erosion (Declercq et al. 2015), and the inability to culture the causative agent on Flavobacterium-specific media such as Anacker-Ordal Agar.

Additionally, the likelihood of incorrect read attribution to known CCB in the NGS analysis is low, as numerous intermediate species were present in the reference database. Furthermore, the outbreaks did not correlate with husbandry factors, occurring in multiple farms that shared only water temperature as a common parameter.

The NGS results also revealed a striking similarity between the bacterial communities in the 'Healthy T0' and 'T1' groups, and no relapses were observed following antibiotic treatment. These findings suggest the possible existence of a previously undescribed fifth member of the CCB group, linked to the *Flavobacterium* genus. This organism may belong to the MDM and be evading conventional bacteriological techniques.

An alternative hypothesis is that the disease results from a mixed population of *Flavobacterium* species rather than a single pathogen and is associated with nonoptimal welfare or altered environmental parameters; however, this scenario appears unlikely.

TABLE 1 | Results of sequence comparisons through ClustalW.

Sequence	*F. columnaris*	*F. covae*	*F. davisii*	*F. oreochromis*	No. sequences
F. bernardetii	93%	90%	89%	92%	58
F. aquicola	92%	92%	91%	92%	> 100
F. hiemivividum	92%	91%	91%	91%	> 100

Note: The first column shows the investigated species (the most important and prevalent according to the confrontation). The second, third, fourth, and fifth columns show the similarity between their V3–V4 fragments of 16S rRNA and the CCB. The sixth column indicates the number of species with higher similarity with the investigated bacterium than with the most similar among the CCB (> 93% for *F. Bernardetii*, > 92% for the others).

We systematically assessed potential environmental contributors (e.g., water quality, husbandry practises) and found no consistent associations with disease onset across sites, except for the stable water temperature (14.5°C–16°C), which is within the normal range for these farming regions.

Moreover, the distinct bacterial signature identified in affected fish, the lack of evidence supporting polymicrobial infection, and the absence of relapses following antibiotic treatment collectively support the hypothesis of a novel pathogenic bacterium within the *Flavobacterium* genus.

To help farmers, veterinarians, and fish health personnel with screening and monitoring activities, it is of fundamental importance to use tools that can provide fast and unbiased results that help decide and take action on different challenges in a time- and cost-efficient manner.

While NGS is a robust tool for both qualitative and quantitative disease investigation, which partially addresses the limitations of MDM, it is currently less effective in supporting decision-making compared to its capabilities in exploration and discovery. This is largely due to its high costs, time-consuming nature, need for bioinformatic interpretation, and the ongoing requirement for high-quality samples to yield reliable results.

To achieve species-level identification and determine the relationship between the bacteria found in this study and the key taxa of interest, the next step would be to use selective culture media and characterise isolated strains through V3–V4 16S rRNA sequencing, prioritising those that best match our candidate taxa. Alternatively, high-depth shotgun metagenomics could provide a more precise taxonomic resolution and offer insights into the metabolic pathways involved in disease manifestation.

Given the current findings, isolating the bacteria associated with the outbreak remains a crucial step in unravelling the disease's pathogenesis, antibiotic resistance profile, and designing effective prevention strategies, including rapid diagnostic tools. This approach will not only clarify the role of these microorganisms in disease progression but also contribute to the development of targeted interventions for future outbreaks.

Author Contributions

Samuele Zamparo: conceptualization, funding acquisition, investigation, writing – original draft, writing – review and editing. **Ginevra Brocca:** investigation, methodology, visualization, writing – original draft, writing – review and editing. **Fabio Marroni:** data curation, formal analysis, methodology, software, visualization, writing – original draft. **Slobodanka Radovic:** data curation, formal analysis, methodology, software, visualization, writing – original draft. **Ciro Castellano:** funding acquisition, investigation, resources. **Diana Torge:** investigation, methodology, visualization, writing – original draft. **Serena Bianchi:** investigation, methodology, visualization, writing – original draft. **David Groman:** methodology, visualization, supervision. **Guido Macchiarelli:** investigation, methodology, visualization, writing – original draft. **Luisa Vera Muscatello:** supervision, visualization. **Donatella Volpatti:** funding acquisition, resources, supervision. **Massimo Orioles:** conceptualization, funding acquisition, supervision, writing – original draft, writing – review and editing.

Acknowledgements

The authors thank Cortinovis Luana, Marsella Andrea, Pretto Tobia, and Toffan Anna from the 'Istituto Zooprofilattico Sperimentale delle Venezie' for the Bacteriological and Virological analyses.

Conflicts of Interest

The authors declare no conflicts of interest.

Data Availability Statement

The datasets generated and analysed during the current study are available in the SRA repository under accession number PRJNA1178272. Scripts and functions used in this work are available at https://github.com/fabiomarroni/SDOM.

References

Avendaño-Herrera, R., V. Gherardelli, P. Olmos, M. G. Godoy, A. Heisinger, and J. Fernández. 2011. "*Flavobacterium Columnare* Associated With Mortality of Salmonids Farmed in Chile: A Case Report of Two Outbreaks." *Bulletin of the European Association of Fish Pathologists* 31: 36–44.

Birlanga, V. B., G. McCormack, U. Z. Ijaz, E. MacCarthy, C. Smith, and G. Collins. 2022. "Dynamic Gill and Mucus Microbiomes During a Gill Disease Episode in Farmed Atlantic Salmon." *Scientific Reports* 12: 16719.

Buermans, H. P., and J. T. den Dunnen. 2014. "Next Generation Sequencing Technology: Advances and Applications." *Biochimica et Biophysica Acta* 1842: 1932–1941. https://doi.org/10.1016/j.bbadis.2014.06.015.

Bullard, S. A., A. McElwain, and C. R. Arias. 2011. "Scanning Electron Microscopy of "Saddleback" Lesions Associated With Experimental Infections of *Flavobacterium Columnare* in Channel Catfish, *Ictalurus Punctatus* (Siluriformes: Ictaluridae), and Zebrafish, *Danio Rerio* (Cypriniformes: Cyprinidae)." *Journal of the World Aquaculture Society* 42: 906–913. https://doi.org/10.1111/j.1749-7345.2011.00527.x.

Buller, N. B. 2014. *Bacteria From Fish and Other Aquatic Animals: A Practical Identification Manual*. 2nd ed. CABI Publishing.

Cattonaro, F., A. Spadotto, S. Radovic, and F. Marroni. 2018. "Effect of Coverage Reduction on Metagenome Shotgun Sequencing Studies." *F1000Research* 7: 1767. https://doi.org/10.12688/f1000research.16804.4.

Clinton, M., A. J. Wyness, S. A. M. Martin, A. S. Brierley, and D. E. K. Ferrier. 2021. "Sampling the Fish Gill Microbiome: A Comparison of Tissue Biopsies and Swabs." *BMC Microbiology* 21: 313. https://doi.org/10.1186/s12866-021-02374-0.

Declercq, A. M., K. Chiers, F. Haesebrouck, et al. 2015. "Gill Infection Model for Columnaris Disease in Common Carp and Rainbow Trout." *Journal of Aquatic Animal Health* 27: 1–11. https://doi.org/10.1080/08997659.2014.953265.

Declercq, A. M., F. Haesebrouck, W. Van den Broeck, P. Bossier, and A. Decostere. 2013. "Columnaris Disease in Fish: A Review With Emphasis on Bacterium-Host Interactions." *Veterinary Research* 44: 27. https://doi.org/10.1186/1297-9716-44-27.

Decostere, A., F. Haesebrouck, and L. A. Devriese. 1998. "Characterization of Four *Flavobacterium Columnare* Strains Isolated From Tropical Fish." *Veterinary Microbiology* 62: 35–45. https://doi.org/10.1016/s0378-1135(98)00196-5.

Dong, H. T., S. Senapin, B. LaFrentz, and C. Rodkhum. 2015. "Virulence Assay of Rhizoid and Non-Rhizoid Morphotypes of *Flavobacterium Columnare* in Red Tilapia, Oreochromis sp., Fry." *Journal of Fish Diseases* 39: 649–655. https://doi.org/10.1111/jfd.12385.

Ferguson, H. W., V. E. Ostland, D. D. MacPhee, J. S. Lumsden, P. J. Byrne, and D. J. Speare. 1995. "'No-Mucus Skin Disease' of Rainbow

Trout, *Oncorhynchus mykiss* (Walbaum): A Case Report." *Journal of Fish Diseases* 18: 49–57. https://doi.org/10.1111/j.1365-2761.1995.tb01265.x.

Hadfield, C. A. 2021. "Bacterial Diseases." In *Clinical Guide to Fish Medicine, Section C Diseases of Fish*, edited by C. Hadfield and L. Clayton, 431–467. Wiley.

Hodneland, K., and C. Endresen. 2006. "Sensitive and Specific Detection of Salmonid Alphavirus Using Real-Time PCR (TaqMan)." *Journal of Virological Methods* 131: 184–192. https://doi.org/10.1016/j.jviromet.2005.08.012.

Hutson, K. S., I. C. Davidson, J. Bennett, R. Poulin, and P. L. Cahill. 2023. "Assigning Cause for Emerging Diseases of Aquatic Organisms." *Trends in Microbiology* 31: 681–691. https://doi.org/10.1016/j.tim.2023.01.012.

Jiao, J. Y., L. Liu, Z. S. Hua, et al. 2021. "Microbial Dark Matter Coming to Light: Challenges and Opportunities." *National Science Review* 8: nwaa280. https://doi.org/10.1093/nsr/nwaa280.

Jonstrup, S. P., S. Kahns, H. F. Skall, T. S. Boutrup, and N. J. Olesen. 2013. "Development and Validation of a Novel Taqman-Based Real-Time RT-PCR Assay Suitable for Demonstrating Freedom From Viral Haemorrhagic Septicaemia Virus." *Journal of Fish Diseases* 36: 9–23. https://doi.org/10.1111/j.1365-2761.2012.01416.x.

LaFrentz, B. R., S. Królová, C. R. Burbick, et al. 2022. "The Fish Pathogen *Flavobacterium columnare* Represents Four Distinct Species: *Flavobacterium columnare*, *Flavobacterium Covae* sp. Nov., *Flavobacterium Davisii* sp. Nov. and *Flavobacterium Oreochromis* sp. Nov., and Emended Description of *Flavobacterium columnare*." *Systematic and Applied Microbiology* 45: 126293. https://doi.org/10.1016/j.syapm.2021.126293.

Leal, J. F., E. B. H. Santos, and V. I. Esteves. 2019. "Oxytetracycline in Intensive Aquaculture: Water Quality During and After Its Administration, Environmental Fate, Toxicity and Bacterial Resistance." *Reviews in Aquaculture* 11: 1176–1194. https://doi.org/10.1111/raq.12286.

Love, M. I., W. Huber, and S. Anders. 2014. "Moderated Estimation of Fold Change and Dispersion for RNA-Seq Data With DESeq2." *Genome Biology* 15: 550. https://doi.org/10.1186/s13059-014-0550-8.

Lu, J., F. P. Breitwieser, P. Thielen, and S. L. Salzberg. 2017. "Bracken: Estimating Species Abundance in Metagenomics Data." *PeerJ Computer Science* 3: e104. https://doi.org/10.7717/peerj-cs.104.

Noga, E. J. 2010. *Fish Disease: Diagnosis and Treatment*, 2nd ed. Wiley-Blackwell.

Orioles, M., M. Galeotti, E. Saccà, et al. 2022. "Effect of Temperature on Transfer of Midichloria-Like Organism and Development of Red Mark Syndrome in Rainbow Trout (*Oncorhynchus mykiss*)." *Aquaculture* 560: 738577. https://doi.org/10.1016/j.aquaculture.2022.738577.

Overturf, K., S. LaPatra, and M. Powell. 2001. "Real-Time PCR for the Detection and Quantitative Analysis of IHNV in Salmonids." *Journal of Fish Diseases* 24: 325–333. https://doi.org/10.1046/j.1365-2761.2001.00296.x.

Rigos, G., D. Kogiannou, F. Padrós, et al. 2021. "Best Therapeutic Practices for the Use of Antibacterial Agents in Finfish Aquaculture: A Particular View on European Seabass (*Dicentrarchus labrax*) and Gilthead Seabream (*Sparus aurata*) in Mediterranean Aquaculture." *Reviews in Aquaculture* 13: 1285–1323. https://doi.org/10.1111/raq.12523.

Sehnal, L., E. Brammer-Robbins, A. M. Wormington, et al. 2021. "Microbiome Composition and Function in Aquatic Vertebrates: Small Organisms Making Big Impacts on Aquatic Animal Health." *Frontiers in Microbiology* 12: 567408. https://doi.org/10.3389/fmicb.2021.567408.

Solden, L., K. Lloyd, and K. Wrighton. 2016. "The Bright Side of Microbial Dark Matter: Lessons Learned From the Uncultivated Majority." *Current Opinion in Microbiology* 31: 217–226. https://doi.org/10.1016/j.mib.2016.04.020.

Soto, E., M. J. Mauel, A. Karsi, and M. L. Lawrence. 2008. "Genetic and Virulence Characterization of *Flavobacterium columnare* From Channel Catfish (*Ictalurus punctatus*)." *Journal of Applied Microbiology* 104: 1302–1310. https://doi.org/10.1111/j.1365-2672.2007.03632.x.

Torge, D., S. Bernardi, G. Ciciarelli, G. Macchiarelli, and S. Bianchi. 2024. "Dedicated Protocol for Ultrastructural Analysis of Farmed Rainbow Trout (*Oncorhynchus mykiss*) Tissues With Red Mark Syndrome: The Skin—Part One." *Methods and Protocols* 7: 37. https://doi.org/10.3390/mps7030037.

Wood, D. E., J. Lu, and B. Langmead. 2019. "Improved Metagenomic Analysis With Kraken 2." *Genome Biology* 20: 257. https://doi.org/10.1186/s13059-019-1891-0.

Zamparo, S., M. Orioles, G. Brocca, et al. 2024. "Novel Insights on Microbiome Dynamics During a Gill Disease Outbreak in Farmed Rainbow Trout (*Oncorhynchus mykiss*)." *Scientific Reports* 14: 17791. https://doi.org/10.1038/s41598-024-68287-w.

Zhou, C., H. Wang, H. Zhao, and T. Wang. 2022. "fastANCOM: A Fast Method for Analysis of Compositions of Microbiomes." *Bioinformatics* 38: 2039–2041. https://doi.org/10.1093/bioinformatics/btac060.

Supporting Information

Additional supporting information can be found online in the Supporting Information section.